PHYSICAL REVIEW D VOLUME 27, NUMBER 7 1 APRIL 1983

Analysis of deep-underground muons

J. W. Elbert
Physics Department, University of Utah, Salt Lake City, Utah 84112

T. K. Gaisser and Todor Stanev*
Bartol Research Foundation of The Franklin Institute, University of Delaware, Newark, Delaware 19711
(Received 2 July 1982)

We compare results of Monte Carlo simulations to results from two deep-underground muon experiments. The primary goal is to obtain information about chemical composition of primary cosmic rays with energies around 10^{14}–10^{15} eV. We also check consistency of the two experiments and study the transverse-momentum distribution of the parent muons.

I. INTRODUCTION

Recently reported data on near vertical muons observed in the Homestake underground detector[1] can be compared with muons under similar slant depths but from large zenith angles. The latter data were obtained some time ago[2] at the shallower Utah muon detector. The data sets overlap and complement each other also in the range of transverse momenta explored, so the comparison of both sets of results with a single calculation seems worthwhile. The Utah data alone have been studied extensively in earlier calculations of a similar type.[3]

Rates of underground muons are sensitive to models of the primary-cosmic-ray spectrum and composition and to properties of hadronic interactions. A number of experimental quantities give useful constraints on the interaction model. First, the muon flux can be studied at a given depth as a function of zenith angle. This can be used to test whether the data show the sec θ dependence expected from muon production by decay of pions and kaons. If detectable fractions of the muons originate from rapidly decaying particles, such as charmed mesons, it would add an isotropic component to the sec θ angular dependence.

A second experimental distribution for which the predictions are sensitive to the interaction model is the decoherence curve. For two "small" muon detectors of areas A_1 and A_2 with a rate of R coincident events per unit time, the decoherence curve is defined as $D(r)=R/A_1A_2$, where r is the separation between the two detectors (r is the separation perpendicular to the direction of the muons). Of course, the decoherence curve can be measured in a large position-sensitive detector by dividing the detector into many "small" detectors (detectors with smaller dimensions than the separation r and the typical separations between the muons). The mean separation of the pairs depends quite directly on the mean transverse momentum of the parent mesons and the distance from the detector to the production point of the muon.

The normalization of the decoherence curve is also of interest. It is sensitive to the spectrum and composition of the primary cosmic rays. The primary composition has different effects on the muon flux and the decoherence curve normalization. The muon flux tends to be dominated by the proton part of the primary composition, while the other nuclei, if present, give very large contributions to the decoherence curve.

A third type of data which is available is the rates of events with n muons in a detector. These rates depend on all the factors mentioned above which influence the normalization and mean separation of the decoherence curve.

We present here a comparison between Monte Carlo calculations and the data from Utah and Homestake. In order to compare the results of the two experiments, we focus on the data from Utah which are at comparable slant depths to the vertical data from Homestake. Because of the large zenith angle, muons observed at Utah have traveled about 2.8 times as far as those at Homestake. Homestake data thus tend to complement the Utah data because large effective separations, which would not be contained in the central Utah detector, can be seen in the Homestake detector because distances are scaled down by a factor of 2.8. There is also a region of overlap between the two data sets. Moreover, the data obtained with an outrigger detector extend the Utah data to large distances, overlapping the full range of the Homestake detector.

The plan of the paper is as follows: Section II describes the details of the simulation and models used. A discussion of the extent to which possible sources of prompt muons could contribute to the measured quantities is given in Sec. III. Section IV deals with the lateral distribution of the muons and Sec. V with the rates of multiple muons. A general discussion and the conclusions are given in Sec. VI. Our results allow us to study the sensitivity of the various observables in underground muon experiments to primary composition. With the present data we are not, however, able to distinguish among a range of reasonable primary compositions.

II. DESCRIPTION OF MODELS AND THE SIMULATION

We consider two standard primary compositions, which bracket a range of other reasonable possibilities to be discussed later. They are the following:

(1) A low-energy (LE) composition[4] with differential spectral index of 2.71 for all species and five mass groups in the ratios

$$p\text{:He:CNO:Mg:Fe}=1\text{:}0.035\text{:}0.0018\text{:}0.0005\text{:}0.000\,15$$

at the same energy per nucleon.

(2) An extrapolation of the result of the Maryland group[5] in which the relative fraction of primary heavy nuclei increases with energy. In this model (MD), the iron-group nuclei have a spectral index of 2.36 and the other groups have an index of 2.71. On a total energy per nucleus basis, the iron group make up about 65% of the primaries above 2 PeV. For consistency with the all-particle spectrum, we assume that all components steepen to a differential slope of 3 at 2 PeV.

The interaction model used assumed total inelastic cross sections to increase with energy and energy independence of the Feynman-x and p_T distributions of produced particles.[6] The K/π ratio was assumed to be $\frac{1}{9}$ and energy independent. The transverse-momentum distribution for pions, integrated over x, was of the form $p_T\exp(-Kp_T)$, with p_T in GeV/c. The "seagull effect" was incorporated, making $\langle p_T\rangle$ dependent on x. For $x<0.2$ the exponent in the p_T distribution was calculated to be $2p_T/(x+\frac{1}{4})$ while for $x>0.2$ we used a constant exponent of $4.44p_T$.

The simulation was performed in three stages. The first one consisted of the cascade simulation itself: a three-dimensional Monte Carlo simulation of atmospheric cascades where the energy and spatial coordinates of every produced muon with energy greater than 1.5 TeV were saved. This portion of the program was run for protons with energy between 2 and 10 000 TeV, divided into ten energy segments. The spectral index in each segment was 2.71 and the number of showers simulated per segment was chosen to provide a sufficient number of muons.

In the second stage of the simulation the muons produced in stage I were propagated through the rest of the atmosphere as well as through the rock to the detector level. The deflection in the Earth's magnetic field was added to the multiple-Coulomb-scattering deflection which was calculated in depth bins corresponding to 5% energy loss. The muon-energy-loss simulation took into account the processes of e^+e^- pair production, bremsstrahlung, ionization loss, and muon nuclear interactions. The output of the second stage consisted of the coordinates of the muons surviving to the level of the detector.

Stage III of the simulation procedure accounted for the detector response to muons and calculated observable values as rates of muons in the detector with multiplicity n, separation distributions between muon pairs, etc., for different primary-cosmic-ray compositions and spectra. The compositions were constructed through proper weighting of the energy segments used in stage I, using superposition to simulate muons generated by primary nuclei heavier than protons.

Although the number of events generated per energy segment was carefully chosen to provide appropriate statistics some calculated quantities still have significant statistical errors. This applies especially to the normalization of the decoherence curve, where the contribution of a single event of very high multiplicity n weights heavily by producing $n(n-1)/2$ pairs.

III. PROMPT MUONS

The muons produced by decay of charm and higher flavors could be of significant importance for the high-energy muon experiments if the production cross section of charmed baryons in the fragmentation region is an appreciable fraction of the Λ production as indicated by some experiments.[7] Prompt muons from leptonic decay of such particles would be weighted heavily in the cosmic-ray experiments with the steeply falling primary spectrum.

In our calculations[8] we assumed that the charmed baryon production is $\frac{1}{4}$ of the Λ production at $\sqrt{s}=25$ GeV and that it has the same Feynman-x dependence $d\sigma/dx\propto(1-x)$. We took

$$\sigma_{\text{charm}}(\text{mb})=0.36\ln(s/80\ \text{GeV}^2)\ , \tag{1}$$

with the argument of the logarithm motivated by the assumed diffractive production. We also assumed that the branching ratio B_μ for a quark flavor to emit a muon and muon neutrino is 10% and called this set of assumptions model 1 for prompt-muon production.

Model 2 has the same branching ratio of $B_\mu=0.1$ and production cross section given by Eq. (1) below $s=4400$ GeV^2 and constant (0.7 mb) above. Model

3 has a production cross section as in model 2 but $B=0.03$.

Model 1 leads to a total $\sigma=6$ mb in pp collisions at 1000 TeV. This generous estimate can be assumed to include some additional production of heavier flavors at high energy. Model 3, alternatively, represents a minimum background for prompt muon production.

Figure 1 compares the integral muon energy spectrum at sea level of ordinary (π and K produced) muons with the spectra of prompt muons produced by the models described above. Prompt-muon production will dominate above 10–100 TeV and could play some role even in the experiments discussed here.

The classic cosmic-ray prompt-muon experiment examines the zenith angle dependence of high-energy muons to look for an isotropic component I_x, superimposed on the background I_{vert} of ordinary muons from decay of pions and kaons. The latter is proportional to sec θ, where θ is the zenith angle of the muon. The muon flux is given by $I_x + I_{\text{vert}} \sec\theta$ for $\theta < 60°$. Note that the background of ordinary muons is suppressed at high energies as the decay path gets longer.

In Fig. 2 we show a comparison of the fitted values of I_x/I_{vert} at different zenith angles as measured in the Utah experiment[9] with the prediction of models 1 and 3. The model predictions represent

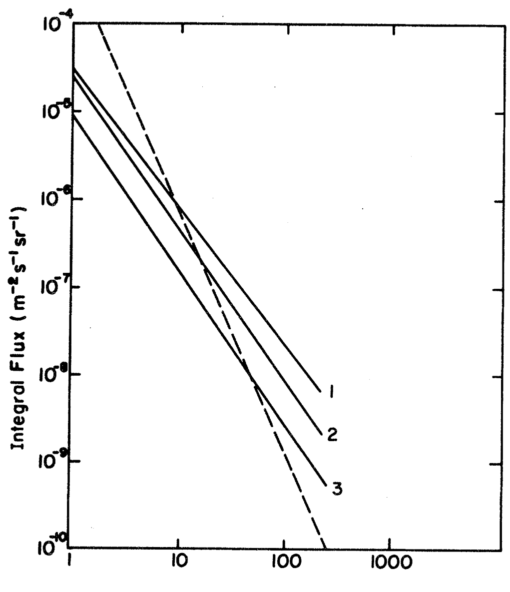

FIG. 1. Comparison of the integral flux of ordinary atomospheric muons (from π and K decays) with that of prompt muons in three different models for production of heavy flavors.

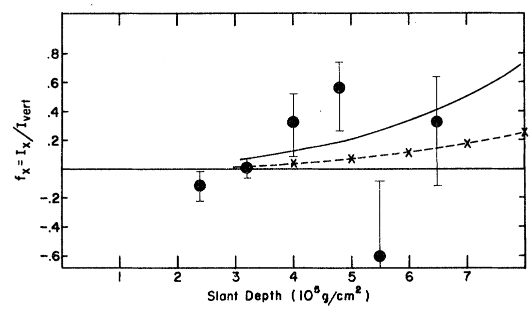

FIG. 2. Comparison of data to model estimates for prompt to ordinary muons obtained from angular dependence of the flux. Solid line shows model 1 and dashed line model 3 for prompt muon production.

the ratio of prompt to total muon fluxes. The present Homestake detector is not designed to measure angular distributions, but Fenyves *et al.*[10] have shown that the data are consistent with no isotropic component for angles out to $\gtrsim 45°$. Comparison with the models of Fig. 1 shows that the Homestake data is also consistent with models 2 and 3 but is on the verge of being inconsistent with model 1.

Since a typical energy for muons to survive to a slant depth of 4200 m water equivalent (m.w.e.) is about 2.3 TeV, even in model 1 prompt muons are a small part of the total flux of muons at this depth. They could, however, play a bigger role in multiples, which on average come from higher primary energy. In Ref. 8 we estimated that for model 1 one in six doubles includes a prompt muon, but this result depends on the assumed composition. If the composition is low in heavy primaries then prompt muons could be relatively more important since ordinary multiples are produced preferentially by heavy nuclei. This estimate was for doubles only, neglecting the significant effect of the finite detector. Moreover, correlations due to the fact that charm and higher flavors are produced in pairs should be taken into account.[11]

IV. LATERAL DISTRIBUTIONS

It is conventional to parametrize the decoherence function in the form $\exp(-r/r_0)$. Table I gives the resulting numbers for r_0. The experimental values of r_0 are about 1.5 times the calculated values. A modification of the interaction model which could produce this effect is the increase of all p_T values by a factor of 1.5. This brings r_0 into agreement with the experimental value. It is also in good agreement with results obtained in independent calculations which were compared with the Utah data.[12] The scaling up of p_T by this factor is not the only way r_0 could be increased. The effect of a high-p_T tail should also be considered.

TABLE I. Calculated and measured decoherence values.

Experiment	Depth (g/cm^2)	θ (deg)	r_0 (calc) (m)	r_0 (expt) (m)	$\frac{r_0(\text{expt})}{r_0(\text{calc})}$
Utah	4000	62.5	7.4	10.1	1.4
Utah	4800	62.5	4.6	7.9	1.7
Homestake	4400	0	2.2	4.4	2.0

In Fig. 3 the calculated decoherence curves for both MD and LE compositions, scaled by 1.5, are compared to the experimental decoherence. The shaded areas cover 1σ from the unexpanded decoherence curve. The expansion by 1.5 is still not sufficient to match the Homestake decoherence. It is difficult to draw conclusions on the composition from the normalization of the decoherence. It is obvious, however, that our standard compositions are limits for the relative amounts of protons and heavy nuclei, which could fit the data.

V. RATES OF MULTIPLE-MUON EVENTS

To obtain the rates R_n of events with exactly n muons in the detector we have simulated the detailed triggering and data collection characteristics of the Homestake detector. In the Utah case we

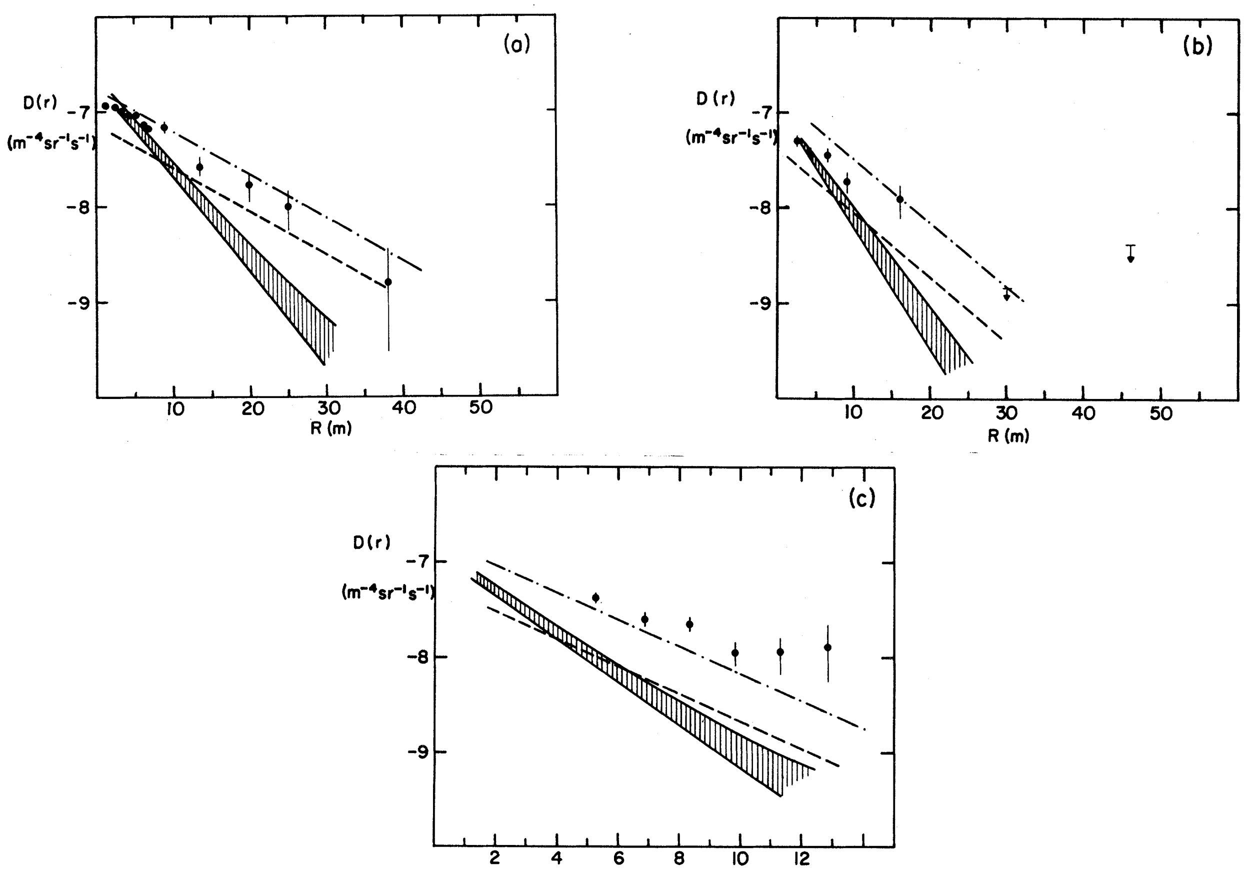

FIG. 3. Comparison between data and calculations for the decoherence curve. Shaded area shows results if the p_T distribution measured at Fermilab and CERN ISR is used. The two lines show results when all distances are scaled up by a factor of 1.5, corresponding to an increased p_T. Dash-dot is for MD composition and dashed line is for LE composition. (a) Utah, 4000 m.w.e., (b) Utah, 4800 m.w.e., and (c) Homestake vertical.

sample events within the 8 m$\times$10 m fiducial detector in terms of which the original data were presented.[2]

Accounting for the detector changes significantly the character of the calculated muon flux. To illustrate this we show in Fig. 4 the relative rates of muons of multiplicity n in an infinite detector at Homestake level and in the Homestake detector itself in the case of the MD composition. The finite detector sharply reduces the observed muon multiplicities. It also decreases the contribution of heavy nuclei to the number of muon groups (as a result of the wider spread of the latter in comparison with the proton produced groups) and correspondingly increases the average primary energy required for the generation of a muon group. The first two lines of each group in Table II give the average energy per nucleon responsible for production of singles, doubles, and triples an infinite detector as well in the Homestake detector for proton and for iron primaries for the MD composition. The next two lines give corresponding values for the Utah detector at both slant depths. The ratio of the contributions of p and of Fe primaries $R(p/\text{Fe})$ to the total observed rates of doubles and triples is also shown.

We find absolute trigger rates about 35% higher than reported at Utah and about 20% below the nominal result at Homestake. Overall rates depend on absolute normalization of the primary spectrum and on details of topography and rock density, which are not yet fully folded into the Homestake results. Moreover, the absolute geometrical acceptance of the Homestake detector is very difficult to calculate. We therefore consider this satisfactory agreement.

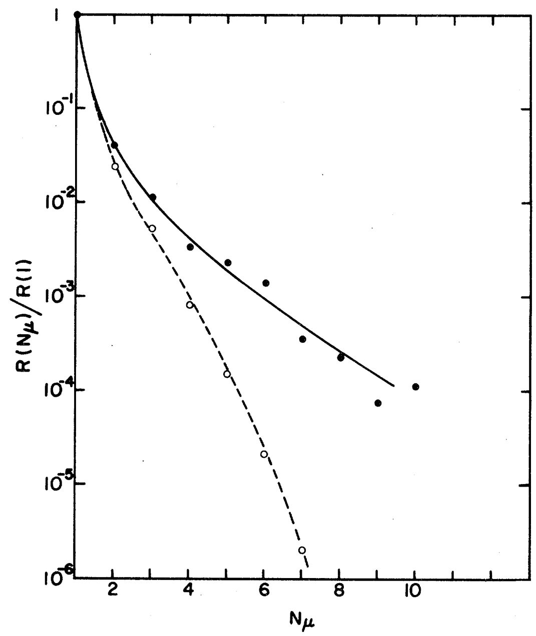

FIG. 4. Calculated rates of multiple muons for $\theta=0°$ at the Homestake depth for MD composition. See Sec. II for definitions. Solid line and points for an "infinite" detector; dashed line and open points for the real detector.

In Tables III–V we compare simulation with data for ratios of rates of multiples to rates of singles in the detector. Results are shown for the unexpanded

TABLE II. Detector response (assuming MD composition). All lateral separations have been scaled up by 1.5. Energies in this table are in TeV/nucleon.

Detector	$\langle E\rangle_p$ (TeV)	$\langle E\rangle_{\text{Fe}}$ (TeV)	$R(p/\text{Fe})$
		Inclusive singles	
Infinite	60	20	13.5
Homestake	80	40	7.7
Utah 4800 m.w.e.	100	50	10.3
Utah 4000 m.w.e.	70	30	9.0
		Inclusive doubles	
Infinite	460	32	0.73
Homestake	800	100	0.63
Utah 4800 m.w.e.	550	80	0.94
Utah 4000 m.w.e.	370	80	1.00
		Inclusive triples	
Infinite	1450	53	0.025
Homestake	1900	170	0.28
Utah 4800 m.w.e.	700	180	0.35
Utah 4000 m.w.e.	420	125	0.28

TABLE III. Comparison of simulations with data for ratios of rates of multiples, to rates of singles in the detector. Utah, 4000 m.w.e. slant depth at 62.5° zenith angle.

	R_2/R_1	R_3/R_1	R_4/R_1
Experiment	0.015±0.002	0.0019±0.0003	0.0004±0.0001
MD (∞ detector)	0.071	0.017	0.011
MD	0.025	0.0061	0.0018
MD (expanded)	0.019	0.0035	0.0012
LE (expanded)	0.014	0.0018	0.0005
$Y2$ (expanded)	0.024	0.0050	0.0020
$Y3$ (expanded)	0.016	0.0023	0.0007
$J19$ (expanded)	0.016	0.0022	0.0006
$J21$ (expanded)	0.022	0.0035	0.0011

MD composition and a set of compositions with expanded p_T. In addition to the standard compositions we show the calculated ratios for two models, suggested for explanation of other high-energy cosmic-ray experiments in Ref. 13 (shown here as $Y2$ and $Y3$) and two other trial compositions, of which the main feature is the decrease of the average mass number for $E > 100$ TeV/nucleon. The relative amounts of nuclei with different mass numbers in these compositions are shown in Figs. 5(a)–5(d). The $Y3$ composition has a fixed magnetic rigidity ($R_c \sim 10^5$ GeV/c) beyond which spectra steepen due to an energy dependent increase in rate of leakage out of the galaxy. The corresponding breaks can be seen in Fig. 5(b) at total energy $=(A/2)R_c$ for $A > 1$. There is also an extragalactic proton component in this model above 10^6 GeV.

We note that the Utah and Homestake detectors respond differently to expansion of the p_T distribution. The introduction of the higher p_T values into the model lowers the probability of obtaining higher multiplicity events in the Utah detectors. In the case of the Homestake detector, however, there is not very much sensitivity of the rates to the p_T value. This is presumably because particles with small separations are not resolved by the detector. As p_T increases, there is compensation for particles "lost" outside the detector by pairs inside the detector becoming separately detectable.

VI. DISCUSSION AND CONCLUSIONS

An inspection of values in Tables III–V shows that we have been unable to find any composition that explains the whole set of experimental data. The MD composition is not in terrible disagreement with the double/single ratio for all experiments. On the other hand, the LE composition explains quite well the triple and quadruple rates in all experiments. Taking into account the somewhat higher mean energies required for production of multiplicities higher than doubles this picture would seem to suggest a composition that is rich in heavy nuclei at energies around 100 TeV/nucleon and close to the LE composition for higher energies.[14]

Three of the compositions ($Y3$, $J19$, and $J21$) have this feature. However, they still fail to explain the experimental data, especially the doubles rate in Homestake. The energy response of the detectors is very broad and every attempt to decrease the

TABLE IV. As in Table III. Utah, 4800 m.w.e. slant depth at 62.5° zenith angle.

	R_2/R_1	R_3/R_1	R_4/R_1
Experiment	0.017±0.004	0.0016±0.0007	
MD (∞ detector)	0.076	0.020	0.006
MD	0.027	0.0051	0.0022
MD (expanded)	0.018	0.0035	0.0016
LE (expanded)	0.013	0.0018	0.0008
$Y2$ (expanded)	0.024	0.0057	0.0027
$Y3$ (expanded)	0.014	0.0022	0.0009
$J19$ (expanded)	0.014	0.0020	0.0008
$J21$ (expanded)	0.019	0.0036	0.0012

TABLE V. As in Table III. Homestake vertical (statistical errors only).

	R_2/R_1	R_3/R_1	R_4/R_1
Experimental	0.040±0.002	0.003±0.001	0.0005±0.0004
MD (∞ detector)	0.040	0.011	0.0033
MD	0.030	0.0038	0.0006
MD (expanded)	0.024	0.0050	0.0008
LE (expanded)	0.015	0.0022	0.0002
$Y2$ (expanded)	0.034	0.0085	0.0020
$Y3$ (expanded)	0.018	0.0028	0.0006
$J19$ (expanded)	0.018	0.0031	0.0002
$J21$ (expanded)	0.028	0.0044	0.0005

amount of triples and higher multiplicities correspondingly lowers the rate of doubles.

Since, in a superposition model, the efficiency for muon-pair production should be proportional to A^2 (Ref. 15) we have paid most attention to the adjustment of the relative amount of protons and iron nuclei in the primary flux. Figure 6 shows the energy dependence of $(\sum_i w_i A_i^2)$, a quantity which should reflect the ability of a composition to produce muon pairs. Actually the finite detector modifies the A dependence and increases the relative contribution of the intermediate groups of nuclei. A good example

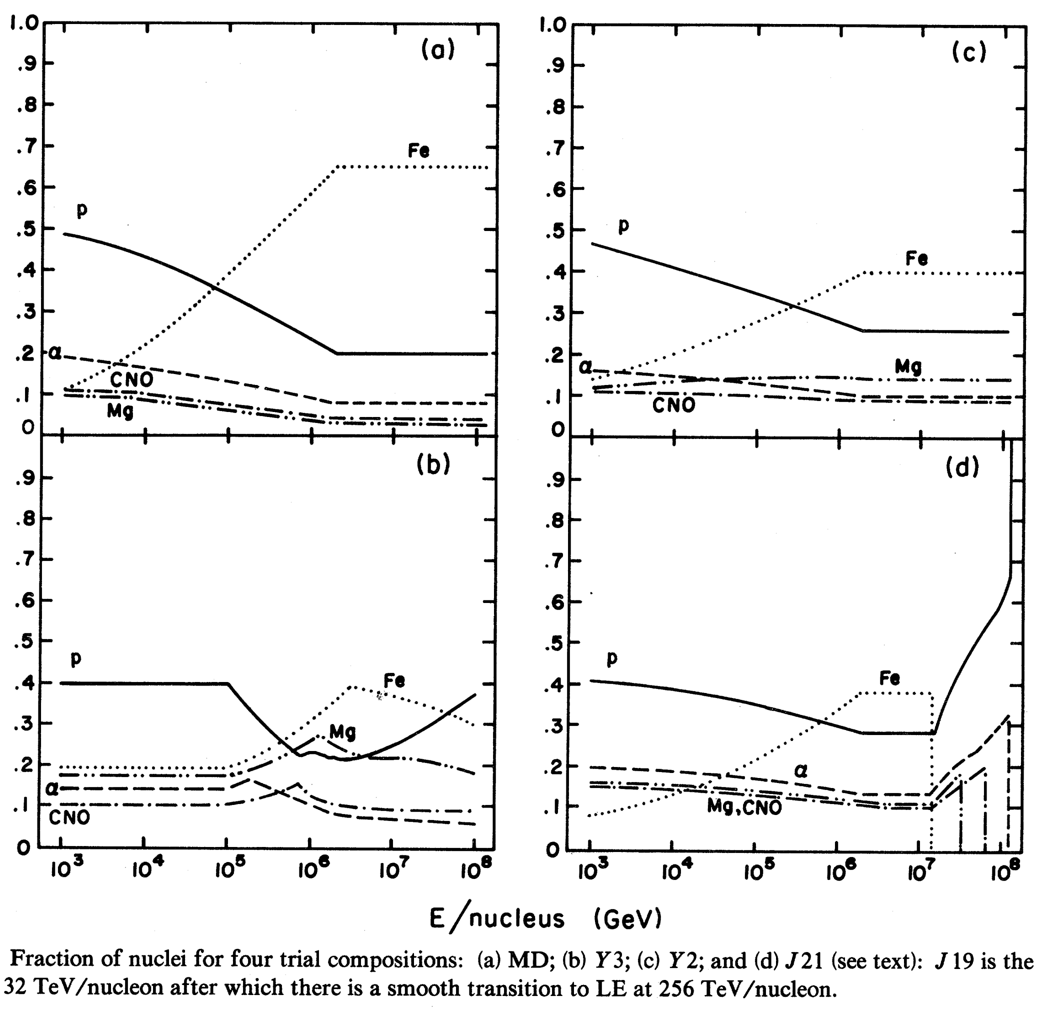

FIG. 5. Fraction of nuclei for four trial compositions: (a) MD; (b) $Y3$; (c) $Y2$; and (d) $J21$ (see text): $J19$ is the same as MD up to 32 TeV/nucleon after which there is a smooth transition to LE at 256 TeV/nucleon.

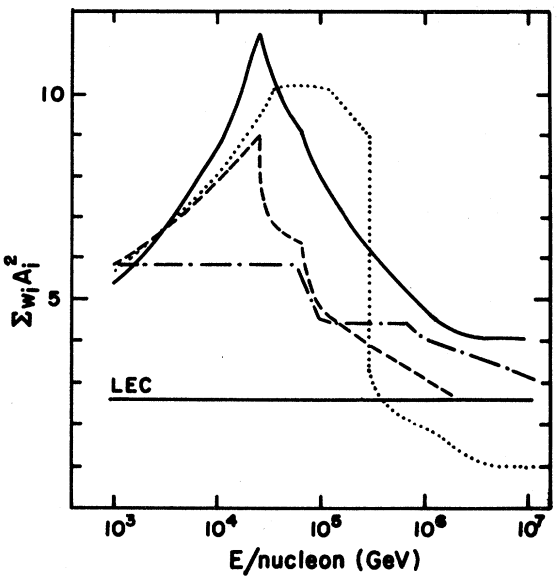

FIG. 6. $\sum w_i A_i^2$ for MD (solid curve); $Y2$ (dashed); $Y3$ (dash-dot) and $J21$ (dotted). The horizontal line is for the energy-independent low-energy composition (LE).

is the $Y2$ composition, which does not look especially attractive on Fig. 6 but still produces more doubles than the MD composition.

$J21$ composition becomes a pure proton one at $E = 10^5$ TeV. The iron-group nuclei are cut off at about 200 TeV/nucleon. We could try to cut the iron earlier in order to match more closely the whole data set, but this will be in contradiction with the indications of the large-emulsion-chamber results on atmospheric interactions.[16]

The results summarized in Tables III–V illustrate the level of sensitivity of deep-underground data on multiple muons to primary composition as well as difficulties associated with the finite detector size, uncertainties in knowledge of rock density and topography (which affect multiples more than singles), and the problem of carrying out an adequate number of simulations given the limitless variety of possible primary compositions.

We are currently developing and applying[17] a semianalytic summary of Monte Carlo results which can be used to survey expectations for multiple muons at various depths and angles, including those of existing and proposed proton decay detectors. We have already used these results to confirm the third line of Table V here. This semianalytic summary should make it possible to explore a wider variety of composition models than can easily be done with the pure Monte Carlo. We will also study the possible advantages of a surface array in coincidence with the underground detector. This would have the advantages of defining the primary energy range responsible for a given type of event and thus move toward the goal of establishing the energy dependence of the composition. For those events seen by both detectors, one would obtain the ratio of multiples to singles for high-energy events. In contrast, the total rate of singles is dominated by the very numerous lower-energy protons whose showers are too small to be seen at the surface. A crucial question to be answered is the rates at which underground/surface coincidences can be observed at various depths and angles.

ACKNOWLEDGMENTS

We wish to thank members of the University of Pennsylvania group for numerous discussions and for furnishing preliminary results from their experiment before publication. This work was supported in part by the National Science Foundation and by the U.S. Department of Energy under DE-AS02-78ER05007.

---

*On leave from the Institute for Nuclear Research and Nuclear Energy, Sofia, Bulgaria.

[1]M. L. Cherry, *et al.*, preceding paper, Phys. Rev. D 27, 1444 (1983).

[2]G. H. Lowe *et al.*, Phys. Rev. D 12, 651 (1975); H. E. Bergeson *et al.*, Phys. Rev. Lett. 35, 1682 (1975).

[3]G. W. Mason *et al.*, in *Proceedings of the Fourteenth International Conference on Cosmic Rays, Munich, 1975,* edited by Klaus Pinkau (Max-Planck-Institut, München, 1975), p. 2943, and Ref. 2.

[4]This composition represents correctly the flux of nuclei in the corresponding mass groups in agreement with most experimental results for energies below 100 GeV/nucleon. See, e.g., J. F. Ormes and P. Freier, Astrophys. J. 222, 471 (1978); M. Simon *et al., ibid.* 239, 712 (1980).

[5]J. A. Goodman *et al.,* Phys. Rev. Lett. 42, 854 (1979). See T. K. Gaisser and G. B. Yodh, Ann. Rev. Nucl. Part. Sci. 30, 475 (1980), for the details of parameters used here. This spectrum is now called MD I by the Maryland group.

[6]R. W. Ellsworth, T. K. Gaisser, and G. B. Yodh, Phys. Rev. D 23, 764 (1981).

[7]For a review see, S. Wojcicki, in *High Energy Physics—1980,* proceedings of the XXth International Conference, Madison, Wisconsin, edited by L. Durand and L. Pondrom (AIP, New York, 1981), p. 1431.

[8]T. K. Gaisser, T. Stanev, and F. Halzen, in *Proceedings of the Topical Workshop on the Production of New Particles in Super-High Energy Collisions, Madison, 1979,* edited by V. Barger and F. Halzen (University of Wisconsin, Madison, Wisconsin, 1979). See also J. W.

Elbert, T. K. Gaisser, and T. Stanev, in *DUMAND 80,* proceedings of the 1980 Symposium, Honolulu, edited by V. J. Stenger (Hawaii DUMAND Center, Honolulu, 1981); F. Halzen, *ibid.*

[9]H. E. Bergesson *et al.,* in *Proceedings of the Thirteenth International Conference on Cosmic Rays, Denver, 1973* (Colorado Associated University Press, Boulder, 1973), p. 1722.

[10]E. Fenyves *et al.,* in *17th International Cosmic Ray Conference, Paris, 1981 Conference Papers* (Centre d'Etudes Nucleaires, Saclay, 1981), Vol. 10, p. 317.

[11]J. W. Elbert, in *Proceedings of the Workshop on Very High Energy Cosmic Ray Interactions,* edited by M. L. Cherry, K. Lande, and R. I. Steinberg (Univ. of Pennsylvania, Philadelphia, 1982), p. 312.

[12]C. Adcock *et al.,* J. Phys. A 3, 697 (1970). See also Bergeson *et al.* (Ref. 2).

[13]R. Cowsik *et al.,* in *17th International Cosmic Ray Conference, Paris, 1981, Conference Papers* (Ref. 10), Vol. 2, p. 120. See also G. B. Yodh, invited talk at the Baltimore meeting of the APS, 1981 (unpublished) and J. A. Goodman *et al,* Phys. Rev. D 26, 1043 (1982).

[14]T. Kitamura, in *17th International Cosmic Ray Conference, Paris, 1981, Conference Papers* (Ref. 10), Vol. 13, p. 361.

[15]J. W. Elbert, in *Proceedings of the DUMAND Summer Workshop, La Jolla, California, 1978,* edited by A. Roberts (Scripps Institution of Oceanography, La Jolla, 1979), Vol. 2, p. 101; J. W. Elbert, in *Sixteenth International Cosmic Ray Conference, Kyoto, 1979 Conference Papers* (Institute of Cosmic Ray Research, University of Tokyo, Tokyo, 1979), p. 405. Strictly, inclusive doubles ($n_\mu \geq 2$) in a infinite detector are proportional to A^2. Multiples in a finite detector include contributions from higher n_μ and so are even more sensitive to A.

[16]T. K. Gaisser and Todor Stanev, in *Proceedings of the Cosmic Ray Workshop on High Energy Interactions and Related Phenomena, La Paz, Bolivia, 1982,* edited by T. K. Gaisser, E. Shibuya, and N. Martinic (University of Campinas, Campinas, S.P., Brazil, to be published).

[17]T. K. Gaisser and Todor Stanev, in *Proceedings of the Summer Workshop on Proton Decay Experiments,* edited by D. S. Ayres (Argonne National Laboratory, 1982), p. 333.